

# BLUE STRAGGLERS, YOUNG WHITE DWARFS, AND UV-EXCESS STARS IN THE CORE OF 47 TUCANAE<sup>1</sup>

FRANCESCO R. FERRARO, NICHÌ D'AMICO, AND ANDREA POSSENTI

Osservatorio Astronomico di Bologna, via Ranzani 1, I-40126 Bologna, Italy; ferraro@apache.bo.astro.it, damico@bo.astro.it, phd@tucanae.bo.astro.it

ROBERTO P. MIGNANI

ESO, Karl Schwarzschild Strasse 2, D-85748 Garching bei München, Germany; rmignani@eso.org

AND

BARBARA PALTRINIERI

Istituto di Astronomia, Università La sapienza, Via G. M. Lancisi 29, I-00161 Rome, Italy; barbara@coma.mporzio.astro.it

Received 2001 May 18; accepted 2001 July 9

## ABSTRACT

We used a set of archived *Hubble Space Telescope*/WFPC2 images to probe the stellar population in the core of the nearby galactic globular cluster (GGC) 47 Tuc. From the ultraviolet (UV) color magnitude diagrams (CMDs) obtained for  $\sim 4000$  stars detected within the Planetary Camera (PC) field of view we have pinpointed a number of interesting objects: (1) 43 blue stragglers stars (BSSs), including 20 new candidates; (2) 12 bright (young) cooling white dwarfs (WDs) at the extreme blue region of the UV-CMD; and (3) a large population of UV-excess (UVE) stars, lying between the BSS and the WD sequences. The colors of the WD candidates identified here define a clean pattern in the CMDs, which define the WD cooling sequence. Moreover, both the location on the UV-CMDs and the number of WDs are in excellent agreement with the theoretical expectations. The UVE stars discovered here represent the largest population of anomalous blue objects ever observed in a globular cluster—if the existence of such a large population is confirmed, we have finally found the long-sought-for population of interacting binaries predicted by the theory. Finally, we have investigated the feasibility of the optical identification of the companions of the binary X-ray sources recently detected by *Chandra* and of binary millisecond pulsars (MSPs) residing in the core of 47 Tuc. Unfortunately, the extreme faintness expected for the MSP companions, together with the huge stellar crowding in the cluster center, prevents statistically reliable identifications based only on positional coincidences.

*Subject headings:* binaries: close — blue stragglers — globular clusters: individual (47 Tucanae) — novae, cataclysmic variables — pulsars: general — stars: neutron

## 1. INTRODUCTION

A large variety of exotic objects have been found to populate the cores of the most concentrated galactic globular clusters (GGCs): blue straggler stars (BSSs), low-mass X-ray binaries (LMXBs), low-luminosity GC X-ray sources (LLGCXs), cataclysmic variables (CVs), and millisecond pulsars (MSPs) (see, e.g., Bailyn 1995). As most of these objects result from interacting binaries (IBs), their formation is strongly favored in the dense stellar environment of a GC, where stellar collisions provide additional channels for the formation and evolution of binary systems, e.g., via tidal captures (Fabian, Pringle, & Rees 1975; Di Stefano & Rappaport 1994) and exchange interactions (Hut, Murphy, & Verbunt 1991).

In this framework, we are performing an extensive search for various by-products of binary evolution in the cores of a sample of GGCs selected on the basis of their photometric properties. In particular, a large population of BSSs (see Ferraro et al. 1997a, 1999b; Paltrinieri et al. 1998) and a few faint ultraviolet (UV) sources suspected to be IBs (see Ferraro et al. 1997a, 1998, 2000a, 2000b) have already been discovered in the framework of an UV survey of a sample of GGCs carried out with the *Hubble Space Telescope* (HST)

(see Ferraro, Paltrinieri, & Cacciari 1999a for a review of the results).

Among GGCs, 47 Tuc is definitely the most promising target for this kind of investigation since it harbors a crowded zoo of stellar species, including BSSs, LMXBs, candidate CVs, and MSPs. In particular, 21 BSSs have been discovered by Paresce et al. (1991, hereafter P91) and confirmed by De Marchi, Paresce, & Ferraro (1992), Guhathakurta et al. (1992), and Gilliland et al. (1998). In addition, 20 MSPs have been detected by Camilo et al. (2000), 13 of which are in binary systems. Recently, Freire et al. (2001) presented accurate timing positions for most of them. Moreover, the cluster hosts a number of unidentified X-ray sources (Verbunt & Hasinger 1998; Grindlay et al. 2001), a dwarf nova (V2) (Paresce & De Marchi 1994; see also Shara et al. 1996), and a suspected interacting binary (V1) found in the error circle of a bright X-ray source by Paresce, De Marchi, & Ferraro (1992) (see also De Marchi, Paresce, & Ferraro 1993). Systematic searches for variability in the core of 47 Tuc have been performed by many groups (see Shara et al. 1996; Edmond et al. 1996; Albrow et al. 2001), also exploiting the large database provided by the survey of Gilliland, which was originally conceived to search for planetary transits (Gilliland et al. 2000).

Here we report on the results of recent *HST* UV observations of the core of 47 Tuc. These observations yielded the discovery of a large population of UV objects (§ 3), which significantly expand the list of the interesting objects

<sup>1</sup> Based on observations with the NASA/ESA *Hubble Space Telescope*, obtained at the Space Telescope Science Institute, which is operated by AURA, Inc., under NASA contract NAS 5-26555.

TABLE 1  
DESCRIPTION OF THE USED DATA SETS

| Date              | Proposal Identification | Filter | $\lambda/\Delta\lambda$ | Number of Exposures | Integration Time (s) |
|-------------------|-------------------------|--------|-------------------------|---------------------|----------------------|
| 1995 Sep 1 .....  | GO-6095                 | F218W  | 2189                    | 4                   | 800                  |
| 1999 Jul 11 ..... | GO-8267                 | F336W  | 3341                    | 6                   | 900                  |
| 1995 Sep 1 .....  | GO-6095                 | F439W  | 4300                    | 2                   | 50                   |

(Tables 2, 3, and 4) known to reside in the core of 47 Tuc and surely will deserve a more detailed study when higher resolution/sensitivity observations and deeper imaging/spectroscopy become available.

In addition, we have used the same data set to search for the optical counterparts to LLGCXs and MSPs in the core

of 47 Tuc. The results of this search and all the related caveats are discussed in section (§ 4).

## 2. OBSERVATIONS AND DATA ANALYSIS

The data set used in the present work consists of a series of public *HST*/WFPC2 exposures mapping the core of the

TABLE 2  
BSS CANDIDATES IN 47 TUC

| BSS Number   | Identification | $m_{F218W}$ | $m_{F336W}$ | $m_{F439W}$ | X      | Y      | G92/E96     |
|--------------|----------------|-------------|-------------|-------------|--------|--------|-------------|
| BSS-1 .....  | 1893           | 15.92       | 15.34       | 14.46       | 556.60 | 400.85 | 172         |
| BSS-2 .....  | 2314           | 17.63       | 16.29       | 15.72       | 498.78 | 325.23 | 206 (AKO 6) |
| BSS-3 .....  | 3084           | 17.99       | 16.76       | 16.21       | 438.14 | 178.80 | ...         |
| BSS-4 .....  | 997            | 17.20       | 16.38       | 15.78       | 421.77 | 556.46 | 302         |
| BSS-5 .....  | 2094           | 16.76       | 16.08       | 15.26       | 392.19 | 365.54 | 299 (V6)    |
| BSS-6 .....  | 3132           | 17.86       | 16.87       | 16.30       | 358.08 | 171.09 | ...         |
| BSS-7 .....  | 3255           | 17.15       | 16.32       | 15.68       | 348.52 | 145.64 | 312         |
| BSS-8 .....  | 2004           | 17.79       | 16.72       | 16.12       | 376.00 | 382.06 | ...         |
| BSS-10 ..... | 1420           | 17.73       | 16.62       | 16.06       | 367.75 | 480.76 | ...         |
| BSS-12 ..... | 1654           | 18.69       | 17.00       | 16.49       | 351.66 | 442.10 | ...         |
| BSS-13 ..... | 2025           | 17.01       | 16.06       | 15.25       | 307.85 | 378.44 | 386         |
| BSS-14 ..... | 1835           | 18.19       | 16.92       | 16.33       | 309.64 | 409.05 | ...         |
| BSS-15 ..... | 694            | 17.12       | 16.29       | 15.65       | 344.68 | 622.69 | 389         |
| BSS-16 ..... | 947            | 17.28       | 16.50       | 15.89       | 332.21 | 565.74 | V12         |
| BSS-18 ..... | 1561           | 16.92       | 16.20       | 15.47       | 308.13 | 459.84 | 398 (V3)    |
| BSS-19 ..... | 1764           | 16.38       | 15.82       | 14.87       | 157.26 | 422.67 | 534         |
| BSS-20 ..... | 2556           | 18.04       | 16.77       | 16.26       | 110.84 | 281.95 | ...         |
| BSS-21 ..... | 642            | 18.45       | 16.90       | 16.41       | 211.47 | 632.92 | ...         |
| BSS-22 ..... | 183            | 17.06       | ...         | 15.24       | 373.60 | 742.95 | 381 (V1)    |
| BSS-23 ..... | 3086           | 15.96       | 15.54       | 14.48       | 262.24 | 178.40 | 399         |
| BSS-24 ..... | 2835           | 18.07       | 17.05       | 16.45       | 127.40 | 227.41 | V10         |
| BSS-25 ..... | 2675           | 16.46       | 15.74       | 14.85       | 712.99 | 257.58 | 32          |
| BSS-26 ..... | 2324           | 19.21       | 17.64       | 17.52       | 451.66 | 323.77 | V11 (AKO 9) |
| BSS-27 ..... | 3212           | 19.22       | 17.85       | 17.30       | 255.84 | 153.44 | ...         |
| BSS-28 ..... | 2947           | 18.56       | 16.65       | 16.05       | 251.63 | 204.62 | ...         |
| BSS-29 ..... | 2712           | 17.63       | 16.79       | 16.23       | 529.18 | 250.89 | ...         |
| BSS-30 ..... | 2637           | 19.02       | 17.41       | 16.85       | 122.77 | 265.71 | ...         |
| BSS-31 ..... | 2364           | 17.90       | 16.00       | 15.45       | 645.27 | 315.88 | ...         |
| BSS-32 ..... | 1901           | 18.51       | 17.30       | 16.78       | 471.27 | 399.25 | ...         |
| BSS-33 ..... | 1838           | 18.10       | 16.57       | 16.01       | 574.08 | 408.72 | ...         |
| BSS-34 ..... | 1819           | 19.26       | 17.52       | 17.04       | 296.37 | 411.62 | ...         |
| BSS-35 ..... | 1603           | 19.34       | 17.10       | 16.63       | 327.81 | 451.06 | ...         |
| BSS-36 ..... | 1393           | 18.94       | 17.61       | 17.17       | 310.02 | 484.39 | ...         |
| BSS-37 ..... | 2121           | 18.79       | ...         | 16.85       | 741.28 | 360.81 | ...         |
| BSS-38 ..... | 1865           | 19.07       | 17.89       | 17.25       | 464.72 | 404.88 | ...         |
| BSS-39 ..... | 1746           | 18.71       | ...         | 16.33       | 642.58 | 425.26 | ...         |
| BSS-40 ..... | 568            | 17.37       | ...         | 15.73       | 460.89 | 644.52 | ...         |
| BSS-41 ..... | 561            | 19.22       | ...         | 16.76       | 542.56 | 645.08 | ...         |
| BSS-42 ..... | 421            | 16.90       | ...         | 15.64       | 149.71 | 680.89 | ...         |
| BSS-43 ..... | 199            | 19.35       | ...         | 17.44       | 64.80  | 739.58 | ...         |
| BSS-44 ..... | 157            | 17.17       | ...         | 15.61       | 734.10 | 753.10 | ...         |
| BSS-45 ..... | 53             | 18.44       | ...         | 16.73       | 324.11 | 780.87 | ...         |
| BSS-46 ..... | 2324           | 19.21       | 17.64       | 17.52       | 451.66 | 323.77 | ...         |

NOTE.—The columns give the BSS number according to the notation of P91, the object identification number, the magnitudes in the three filters, and the object coordinates in PC pixels, as measured relative to the F218W image reference frame. The last column gives the identifications found in the literature.

TABLE 3  
YOUNG WHITE DWARF CANDIDATES IN 47 TUC

| WD Number   | Identification | $m_{F218W}$ | $m_{F336W}$ | $m_{F439W}$ | $X$    | $Y$    |
|-------------|----------------|-------------|-------------|-------------|--------|--------|
| WD-1 .....  | 3561           | 17.41       | ...         | 19.56       | 780.63 | 78.47  |
| WD-2 .....  | 302            | 18.13       | 19.60       | 20.64       | 358.87 | 713.66 |
| WD-3 .....  | 626            | 18.70       | 20.01       | 21.32       | 395.86 | 635.04 |
| WD-4 .....  | 234            | 19.19       | ...         | 21.35       | 201.56 | 733.14 |
| WD-5 .....  | 3036           | 19.26       | 20.52       | 21.60       | 364.93 | 186.49 |
| WD-6 .....  | 2468           | 19.51       | 20.57       | 21.49       | 357.58 | 299.51 |
| WD-7 .....  | 111            | 19.53       | ...         | 21.74       | 304.96 | 765.47 |
| WD-8 .....  | 728            | 19.56       | 21.10       | 21.50       | 414.00 | 614.64 |
| WD-9 .....  | 945            | 19.80       | ...         | 21.97       | 588.24 | 565.99 |
| WD-10 ..... | 3259           | 19.82       | 20.84       | 21.95       | 427.11 | 144.16 |
| WD-11 ..... | 2716           | 19.97       | 21.44       | 22.25       | 404.79 | 250.14 |
| WD-12 ..... | 3251           | 20.06       | 21.26       | 21.93       | 687.62 | 146.26 |

NOTE.—Columns are as in Table 2.

cluster 47 Tuc, taken through the filters F218W, F336W, and F439W. The observing epochs, the filter mean wavelength and width, the integration times, and the number of exposures are summarized in Table 1. The images have been retrieved from the public *HST* archive after the on-the-fly recalibration with the most recent reference files and tables. Images taken through the same filter have been combined and cleaned of cosmic-ray hits using the automatic WFPC2 archive association procedure. In all the selected observations, the core of 47 Tuc was roughly centered on the Planetary Camera (PC) chip, which has the highest angular resolution ( $0''.045 \text{ pixel}^{-1}$ ). We thus decided to focus our analysis on the PC frames only. Note that the F336W images have been taken at a different epoch and with a different telescope roll angle with respect to the F218W/F439W data sets. For this reason, they cover only  $\sim 70\%$  of the PC field of view imaged in the other two filters. The standard procedure described in Ferraro et al. (1997a) was adopted. In short, in order to perform a deep search for faint UV objects we used the combined F218W image (with an equivalent total exposure time of 3200 s) as the reference frame for object detection. The same image was also used as a reference for the frame registration. The photometric reductions have been carried out using ROMAFOT (Buonanno et al. 1983), a package specifically developed to perform accurate photometry in crowded fields. The object list derived from the F218W image was then matched to the corresponding ones obtained from the F336W and F439W

images. A final catalogue with the instrumental magnitude in each filter and coordinates has been compiled for all the identified stars. The instrumental magnitudes were finally transformed to the STMAG photometric system using Table 9 by Holtzman et al. (1995).

### 3. RESULTS AND DISCUSSION

Figure 1 shows the  $(m_{F218W}, m_{F218W} - m_{F336W})$  color magnitude diagram (CMD) obtained from the photometry of more than 4000 stars identified in the PC field of view of the combined F218W image. As it can be seen, the overall morphologies of the branches in this diagram are deformed with respect to the classical  $(V, B - V)$ -plane. For clarity, the main evolutionary sequences are labeled in the diagram (see also Fig. 1 in Ferraro, Paltrinieri, & Cacciari 1999a). Figure 2 shows the  $(m_{F218W}, m_{F218W} - m_{F439W})$  CMD, where the F439W detections have been included.

As expected, the cluster emission at these wavelengths is dominated by hot stars. In particular, since 47 Tuc is a metal-rich cluster with essentially a red horizontal branch (HB), hot HB stars are missing, and the brightest population turns to be composed of BSSs. Schematically, two prominent features appear in Figure 1 and are fully confirmed in the CMD of Figure 2: (1) the population of BSSs (*open circles*), which defines a clean sequence spanning  $\sim 3.5$  mag and is reminiscent of the sequences already observed in other UV-CMDs such as, e.g., M3 (Ferraro et al. 1997a) and M80 (Ferraro et al. 1999b); and (2) the large number of

TABLE 4  
BRIGHT UV-EXCESS STARS (UVES) IN 47 TUC

| UVE Number   | Identification | $m_{F218W}$ | $m_{F336W}$ | $m_{F439W}$ | $X$    | $Y$    |
|--------------|----------------|-------------|-------------|-------------|--------|--------|
| UVE-1 .....  | 247            | 17.34       | ...         | 17.96       | 290.15 | 730.87 |
| UVE-2 .....  | 1798           | 18.05       | 18.03       | 17.16       | 303.81 | 416.16 |
| UVE-3 .....  | 2676           | 18.52       | 18.89       | 19.61       | 510.36 | 256.90 |
| UVE-4 .....  | 1414           | 18.77       | 19.77       | 20.33       | 327.73 | 481.32 |
| UVE-5 .....  | 1406           | 19.35       | 20.09       | 20.25       | 110.73 | 483.36 |
| UVE-6 .....  | 1046           | 19.50       | 20.93       | 20.81       | 454.11 | 546.51 |
| UVE-7 .....  | 3462           | 19.63       | 20.92       | 20.15       | 156.73 | 98.93  |
| UVE-8 .....  | 3378           | 19.95       | 19.98       | 19.13       | 667.83 | 119.54 |
| UVE-9 .....  | 225            | 20.13       | ...         | 19.64       | 122.93 | 735.11 |
| UVE-10 ..... | 2388           | 20.22       | 21.65       | ...         | 682.81 | 310.62 |
| UVE-11 ..... | 1907           | 20.26       | 20.50       | 19.97       | 263.85 | 398.23 |

NOTE.—Columns are as in Tables 2 and 3.

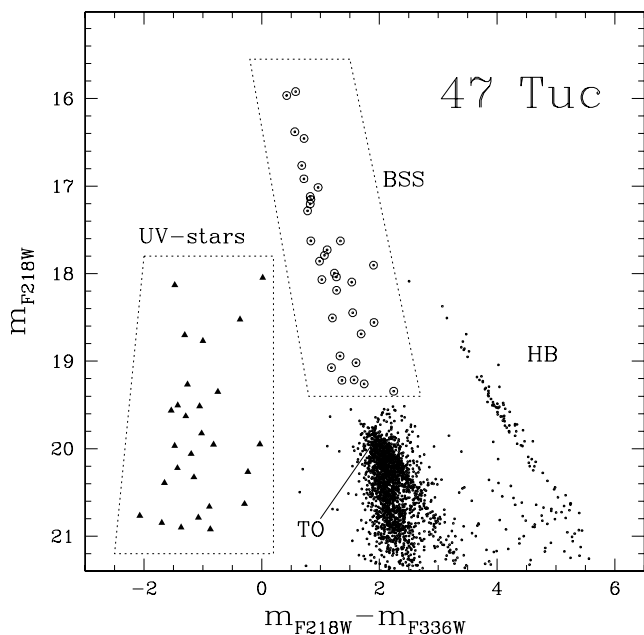


FIG. 1.—( $m_{F218W} - m_{F336W}$ ,  $m_{F218W}$ ) CMD obtained from the photometry of more than 4000 stars detected in the Planetary Camera (PC) field of view. BSSs (see Table 2) are highlighted by large open circles, while the population of UV-stars is plotted as filled triangles. The main evolutionary sequences are labeled.

UV-excess stars (*filled triangles*), which populate the extreme blue region of the diagram ( $m_{F218W} - m_{F336W} < 0$ ). Although the observations presented here span three different epochs, an independent search for variability is beyond the aims of this paper, and we refer to the extensive work by

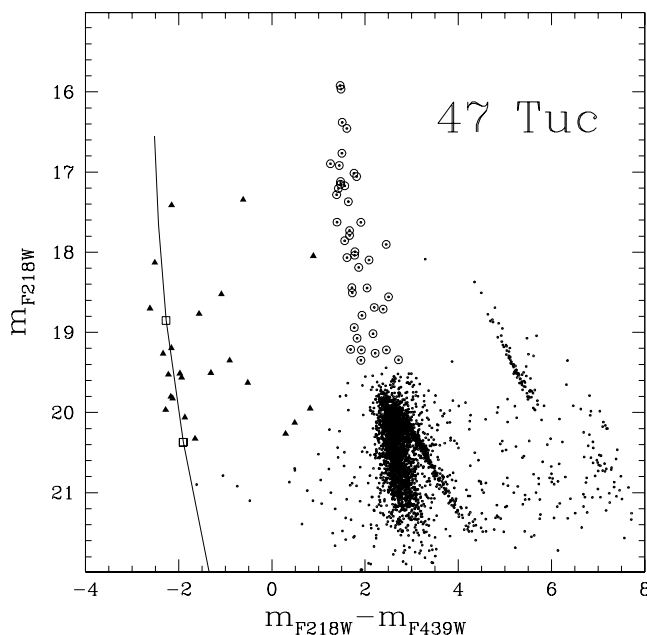


FIG. 2.—( $m_{F218W}$ ,  $m_{F218W} - m_{F439W}$ ) CMD for the same stars shown in Fig. 1. As in Fig. 1, BSSs (see Table 2) are highlighted by large open circles and the population of UV-stars have been plotted as filled triangles. The theoretical WD cooling sequence, computed using the Wood (1995) models, has been overplotted to the data. The two open squares along the WD cooling sequence mark the location of 3 and 13 million year old cooling WDs.

Shara et al. (1996), Edmonds et al. (1996, hereafter E96) and Albrow et al. (2001) in order to check for the variability of the UV objects found in this work.

In the following, we will describe and discuss separately the results of our analysis of these peculiar populations.

### 3.1. Blue Straggler Stars

The presence of BSSs in the core of 47 Tuc has been well known since the pioneering UV observations performed with the Faint Object Camera (FOC) by P91, who discovered 21 BSSs. Most of these identifications are now confirmed by the CMDs shown in Figure 1 and Figure 2, which unveil a total of 43 BSSs with  $m_{F218W} < 19.4$ . Magnitudes and positions for these objects are listed in Table 2. All the coordinates are in PC pixel units ( $0''.045 \text{ pixel}^{-1}$ ) and have been measured in the F218W image reference frame. In Table 2 we adopted the BSS identification code (BSS number) originally used by P91, and we followed this numeration for the other candidates successively discovered by Guhathakurtha et al. (1992, hereafter G92) and E96, as well as for the additional 20 new candidates discovered in the present work. The original identification number by G92 is also listed in the last column, together with the one used by E96 to flag variable objects (namely, V1, V3, V6, V10, V11, and V12). Some of these stars have been successively studied by Gilliland et al. (1998). In particular, V10 (our BSS-24) was classified as an eclipsing variable by E96, while V12 (our BSS-16) was suggested to be a low-amplitude SX Phe variable in a binary system. On the basis of its light-curve shape, V11<sup>2</sup> (our BSS-26) was classified by E96 as an Algol eclipsing binary with a period of  $\sim 1.1$  days. The true nature of V11 is not completely understood. Indeed, while the CMD presented by E96 shows this object as “located near the main-sequence turn-off,” our photometry shows that it is in the BSS region. In addition, its light curve is known to show anomalous features such as, e.g., the rapid brightening detected by Minniti et al. (1997).

Only three BSSs discovered by P91 (namely, BSS-9, BSS-11, and BSS-17) have not been confirmed as BSSs by our criteria. In particular, BSS-11 is located in the region between the cluster turn-off (TO) and the BSS sequence in Figure 2, but it is below the threshold assumed here ( $m_{F218W} = 19.4$ ). BSS-9 (No. 2800 in our list) is the object at  $m_{F218W} \sim 18.1$  and color ( $m_{F218W} - m_{F439W}$ )  $\sim 3.3$  located between the BSS sequence and the HB. BSS-17 (No. 1798 in our list) has been classified as UV-excess star (UVE-2; see § 3.3) since its location in the CMD ( $m_{F218W} \sim 18.05$ ;  $(m_{F218W} - m_{F439W}) \sim 0.9$ ) is significantly bluer than that of the BSS sequence.

### 3.2. Young White Dwarfs

The extended color baseline provided by the CMD in Figure 2 allows us to further investigate the nature of the UV-excess stars identified in Figure 1. In particular, we note how the bluest side of the UV-excess star distribution seems to define a sort of sequence. This would suggest that at least part of the UV-excess stars could be white dwarfs, according with the previous findings by Paresce, De Marchi, & Jędrzejewski (1995). To check this hypothesis we have computed the expected location of the WD cooling sequence in the ( $m_{F218W}$ ,  $m_{F218W} - m_{F439W}$ ) CMD. To do this, we ran

<sup>2</sup> Also known as AKO 9, as named in the original work by Auriere, Koch-Miramond, & Ortolani (1989).

the theoretical cooling sequence for  $0.5 M_{\odot}$  hydrogen-rich WDs (Wood 1995) through the standard IRAF simulation package *synphot* in order to derive the UV-colors and magnitudes for the theoretical WD sequence. A reddening of  $E(B-V) = 0.04$  in the direction of 47 Tuc was assumed. The computed WD sequence is overplotted to the data in Figure 2. As can be seen, the cooling sequence nicely fits the bluest side of the UV-excess distribution and fully supports the conclusion that about half of the UV-excess stars detected in the core of 47 Tuc are indeed WDs. In addition, by comparing the observed WD distribution with the expected location of 3 and 13 million year old cooling WDs (marked by the two open squares along the WD cooling sequence in Fig. 2), we can conclude that the WD population discovered here basically consists of very young objects.

Though the sample presented in Figures 1 and 2 is surely affected by incompleteness at least at the faint end of the sequence ( $m_{F218W} > 20.5$ ), we can try to perform a first-order test to check whether the number of the candidate bright WDs observed in the central region of 47 Tuc is in agreement with the theoretical expectations. To do this, we computed (in accordance with the suggestion by Richer et al. 1997) the number of WD expected in the PC field of view by comparison with the observed number of a tracer population with a known lifetime (as the HB). Taking into account that in the field of view of the PC we observed  $\sim 100$  HB stars, and assuming the HB lifetime  $t_{HB} = 10^8$  yr (Renzini & Fusi Pecci 1988), we derive from their equation (1) the following relation for our sample:

$$N_{WD}(< m_{F218W}^*) = 10^{-6} t_{cool}(< m_{F218W}^*). \quad (1)$$

Here  $N_{WD}(< m_{F218W}^*)$  is the number of WDs brighter than magnitude  $m_{F218W}^*$  and  $t_{cool}(< m_{F218W}^*)$  is the corresponding cooling time in years. According to the Wood's (1995) models,  $t_{cool}(m_{F218W} < 18.9) \sim 3 \times 10^6$  yr and  $t_{cool}(m_{F218W} < 20.4) \sim 1.3 \times 10^7$  yr. Thus, equation (1) predicts  $N_{WD}(m_{F218W} < 18.9) \sim 3$  and  $N_{WD}(m_{F218W} < 20.4) \sim 13$ . Since from Figure 2 we count three and 12 WDs brighter than  $m_{F218W} = 18.9$  and 20.4, respectively, we can conclude that the agreement with the theoretical prediction turns out to be exceptionally good. Thus, we can reasonably assume that all the objects with color  $m_{F218W} - m_{F439W} < -1.6$  are young cooling WD candidates.

Magnitudes, colors, and positions for these stars are listed in Table 2.

### 3.3. UV-Excess stars

Although about half of the UV-excess stars detected in the core of 47 Tuc turn out to be young cooling WDs, there is still a significant number of objects in Figure 2 lying between the BSS sequence and the WD cooling sequence. A zoom of the  $(m_{F218W}, m_{F218W} - m_{F439W})$  CMD is shown in Figure 3, where we have now marked with large empty triangles the WD candidates identified in the previous section and listed in Table 3. As it can be seen from Figure 3, there are at least a dozen UV-excess stars (*filled triangles*) lying between the WD and the BSS sequence. In the following, we refer to these objects as UV-excess (UVE) stars.

The identification numbers, magnitudes, and positions for the 11 brightest ( $m_{F218W} < 20.5$ ) UVE stars are listed in Table 4. UVE-3 has been identified with the blue object V1 (Paresce et al. 1992, hereafter PDF92), which is now clearly confirmed to be an object with strong UV emission. UVE-2

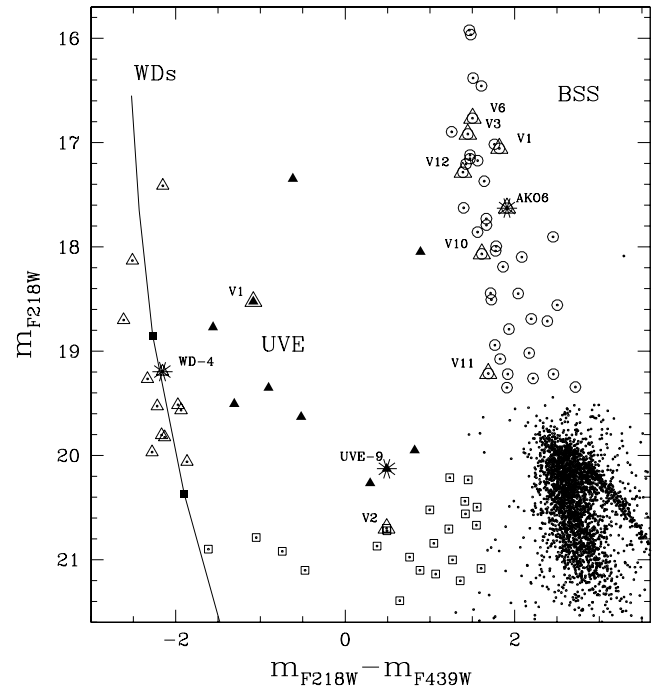


FIG. 3.—Zoom of the  $(m_{F218W}, m_{F218W} - m_{F439W})$  CMD of Fig. 2 showing in more detail the nature of the blue populations in the core of 47 Tuc. BSSs (see Table 2) are highlighted by large open circles, with variables further highlighted by large empty triangles and labeled with their names. WD candidates (see Table 3) are plotted as open triangles. The theoretical WD cooling sequence from Wood's (1995) models has been overplotted to the data (as in Fig. 2), with the location of 3 and 13 million year old cooling WDs now marked by filled squares. Bright UVE stars (see Table 4) are plotted as filled triangles. The presence of a large population of faint UVE stars (*open squares*) is also shown in the figure. Peculiar objects are highlighted by a larger open triangles and labeled with their names. The three blue objects (namely, WD-4, BSS-2 (AKO 6), and UVE-9) that have been found to be close to the three binary MSP (see Table 5) are marked with a large asterisks and labeled with their names.

was originally classified as a BSS (BSS-17) by P91. However, this object is bluer than the BSS sequence, evidence that is also confirmed by previous CMDs of the field (see Fig. 5 by De Marchi et al. (1993), where it clearly stands out from the BSS sequence). UVE-2 is also the variable PC1-V36 discussed by Albrow et al. (2001) and classified as a semidetached binary.

In a recent review, Ferraro et al. (2000b) listed 10 UVE objects (associated with LLGCXs) detected in the core of six GGCs. The population discovered here is much larger than that previously found in any GGC (see Paresce et al. 1991; Paresce & De Marchi 1994; Shara & Drissen 1995; Cool et al. 1995, 1998; Ferraro et al. 1997b, 2000a, 2000b). Moreover, although we conservatively listed in Table 4 only the 11 brightest UVE sources, a population of faint ( $m_{F218W} > 20.5$ ) UVE candidates (*open squares*) is clearly visible in Figure 3, with more than 30 UVE sources counted down to  $m_{F218W} \sim 21.3$ . Unfortunately, the faintness of these objects in all the images prevents firm assessment of their colors. Among the faint UVE stars, we have identified the dwarf nova V2 discovered by Paresce & De Marchi (1994) and the blue variable V3 (suspected to be a CV) discovered by Shara et al. (1996). V2 (No. 5400 in our list) appears to be in a quiescent state at the epoch covered by the present observations, as it is quite faint ( $m_{F218W} = 20.7$  and  $m_{F439W} = 20.2$ ) in both the F218W and F439W images. Also the vari-

able V3 (No. 713 in our list) appears to be faint at the epoch of the observations: it is one of the faintest objects in the UV region of the CMD shown in Figure 1, and it is not visible in the F439W images.

From the number of bona fide identifications and likely candidates pinpointed by our UV-CMDs, we conservatively conclude that *there is a clear indication of the existence of a large population of faint UVE stars in the core of 47 Tuc*. This conclusion is supported by additional, independent, observations. While we were writing this paper, a work by Knigge et al. (2001) reported on the possible detection of a large population of UVE stars ( $\sim 30$ ) in the core of 47 Tuc from far-ultraviolet photometric and spectroscopic *HST*/STIS observations. The availability of a spectroscopic analysis suggested that these stars (or at least part of them) could be CVs. If this is the case, the UVE objects discovered here could represent the brightest extension of the long-searched-for population of CVs predicted by the models (see Di Stefano & Rappaport 1994) and never found by previous observations.

However, alternative evolutionary scenarios exist, which can produce objects populating the same region of the CMD. For instance, Edmonds et al. (1999) suggested that at least one UVE star found in the center of NGC 6397 (Cool et al. 1998) is actually a low-mass helium WD resulting from the stripped core of a red giant (Castellani & Castellani 1993).

#### 4. ABSOLUTE POSITIONS: LIMITS TO THE SEARCH OF OPTICAL COUNTERPARTS TO X-RAY SOURCES AND MSP COMPANIONS

Most of the exotic objects (BSSs, LMXBs, CVs, and MSPs) hosted in the core of GGCs are thought to result from the evolution of various kinds of binary systems. In particular, when a binary system contains a compact object (like a neutron star or a white dwarf) and a close enough secondary, mass transfer can take place, producing an IB. The streaming gas, its impact on the compact object, and the presence of an accretion disk can give such systems observational signatures that make them stand out above ordinary cluster stars. These signatures include X-ray emission, significant radiation in the ultraviolet (UV), emission lines, or rapid time variations. For this reason, the study of peculiar objects usually benefits from a comprehensive multiwavelength approach.

In the case of the UVE stars found in other GGCs, some were found coincident with X-ray sources (Ferraro et al. 1997b, 2000b), while others, such as the ones discovered by Cool et al. (1995) in NGC 6397, by Carson et al. (1999) in  $\omega$ -Cen, and by Ferraro et al. (2000a) in the core of NGC 6712, were found to exhibit significant H $\alpha$  emission. These multiwavelength observations allow one to classify UVE stars as high-confidence IB candidates and/or probable CVs. For this reason, it is particularly interesting here to investigate possible associations between the blue populations (BSSs, WDs, and UVE stars) and some of X-ray sources and MSP companions that are known to harbor in the core of 47 Tuc.

Since the first guess to claim an optical identification is based on the positional coincidence, X- and Y-pixel positions of the objects detected in the PC have been converted to R.A. and decl. using the task *metric* in the IRAF/STSDAS package, which also accounts for the geometric

distortions of the PC. Of course, the accuracy on the final coordinates is entirely dominated by the intrinsic error on the absolute coordinates of the GSC1.1 (Guide Star Catalog) stars (Lasker et al. 1990), which are used both to point *HST* and to compute the astrometric solution in the focal plane. According to the current estimates, the mean uncertainty on the absolute positions quoted in the GSC1.1 is  $\approx 1''.5$  ( $3\sigma$  level of confidence). Thus, we conservatively assume  $\sim 2''$  as the global error on the absolute positions of our objects.

Note that such an estimate is consistent with the average difference between the absolute positions of the same set of stars, as measured in independent *HST* pointings. For instance, G92 measured the absolute position of its star *E* to be R.A.(2000)<sub>G92</sub> = 00<sup>h</sup>24<sup>m</sup>05<sup>s</sup>.33 and decl.(2000)<sub>G92</sub> =  $-72^\circ 04' 54''.46$ , while star No. 2187 in our catalog turns out to be at R.A.(2000) = 00<sup>h</sup>24<sup>m</sup>04<sup>s</sup>.92 and decl.(2000) =  $-72^\circ 04' 54''.25$ , i.e., at  $2''$  from the G92 determination, which fully confirms the uncertainty estimated above.

#### 4.1. X-Ray Sources

Verbunt & Hasinger (1998, hereafter VH98) have recently reanalyzed all the *ROSAT*/HRI images of 47 Tuc obtained in the recent years and finally produced a list of accurate positions and fluxes for nine X-ray sources detected in the cluster core. However, while we were writing this paper Grindlay et al. (2001, hereafter G01) reported the discovery of additional  $\sim 100$  X-ray sources detected from *Chandra* observations. This catalog, listing 108 X-ray sources with  $L_X < 10^{30.5}$  ergs s<sup>-1</sup>, represents the largest and most complete X-ray source catalog ever published in 47 Tuc. For this reason, in the following, we will adopt Table 1 of G01 as a reference list for the positions of X-ray sources in 47 Tuc. Among these, 36 *Chandra* sources fall within the field of view of the PC.

In order account for R.A./decl. offsets between the *HST* coordinate system and the *Chandra* one, we have converted the coordinates listed in Table 1 of G01 in PC pixels using the WFPC2 astrometric solution, and we have shifted the G01 catalog to match the position of the *Chandra* source W46 (X9 in VH98) with the one of its putative counterpart UVE-3 (V1 in PDF92). The choice of the V1/X9 pair as a fiducial position reference is justified by the work of many authors (see, e.g., Geffer, Auriere, & Koch-Miramond 1997 and VH98), which confirms the physical association between the two objects. The shift between the two coordinate systems was admittedly small:  $\delta X = 1''$  ( $\sim 20$  PC pixels) and  $\delta Y = 0''.1$  ( $\sim 2$  PC pixels).

After registering the objects coordinates on a unique reference grid, we cross-correlated the positions of the X-ray sources with the ones derived here for the blue objects. In this way we found an acceptable ( $d < 1''.5$ ) positional coincidence for at least 25 X-ray sources. The identification of all the possible optical counterparts to the X-ray sources of G01 are listed in Table 5, while their positions in the UV CMD are marked in Figure 4. Since we intend to use Table 5 as a working progress list and not a definitive counterparts catalog, in some cases we listed two UV-objects as possible counterparts to a single X-ray source (see the cases of W28, W55, W80, and W98).

It is interesting to note that at least 12 possible optical counterparts to the X-ray sources are faint UVE stars, suggesting, once more, the existence of a large population of faint IBs in the core of 47 Tuc. We confirm the possible

TABLE 5  
*Chandra* X-RAY SOURCES AND ASSOCIATED BLUE OBJECTS

| X-Name     | Name | $m_{F218W}$ | $m_{F336W}$ | $m_{F439W}$ | $X$    | $Y$    | $d$  | Other Names        |
|------------|------|-------------|-------------|-------------|--------|--------|------|--------------------|
| W15 .....  | 2452 | 20.72       | ...         | 20.23       | 69.01  | 302.93 | 1".4 | faint UVE          |
| W19 .....  | 234  | 19.19       | ...         | 21.35       | 201.56 | 733.14 | 0".9 | WD-4               |
| W24 .....  | 1176 | 20.56       | ...         | 19.14       | 236.01 | 521.26 | 1".4 | faint UVE          |
| W27 .....  | 716  | 20.66       | 21.55       | ...         | 346.74 | 617.20 | 0".0 | X10, V3            |
| W28 .....  | 2800 | 18.09       | 15.58       | 14.80       | 335.29 | 233.99 | 1".5 | BSS-9              |
| W28 .....  | 3066 | 21.17       | ...         | 18.92       | 334.03 | 181.80 | 1".2 | faint UVE          |
| W29 .....  | 1408 | 19.55       | 18.04       | 17.55       | 361.41 | 482.70 | 0".1 | faint BSS          |
| W30 .....  | 5400 | 20.70       | 19.41       | 20.21       | 340.85 | 325.13 | 0".1 | X19, V2            |
| W31 .....  | 3255 | 17.15       | 16.32       | 15.68       | 348.52 | 145.64 | 0".4 | BSS-7              |
| W34 .....  | 1046 | 19.50       | 20.93       | 20.81       | 454.11 | 546.51 | 1".3 | UVE-6              |
| W36 .....  | 2324 | 19.21       | 17.64       | 17.52       | 451.66 | 323.77 | 0".1 | BSS-26, AKO 9, V11 |
| W37 .....  | 1865 | 19.07       | 17.89       | 17.25       | 464.72 | 404.88 | 0".5 | BSS-38             |
| W39 .....  | 2314 | 17.63       | 16.29       | 15.72       | 498.78 | 325.23 | 1".5 | BSS-2, AKO 6       |
| W42 .....  | 2676 | 18.52       | 18.89       | 19.61       | 510.36 | 256.90 | 0".0 | UVE-3, X9, V1      |
| W44 .....  | 2907 | 21.58       | ...         | 20.00       | 531.93 | 212.76 | 1".5 | faint UVE          |
| W47 .....  | 3611 | 21.54       | ...         | 19.77       | 558.48 | 68.68  | 0".9 | faint UVE          |
| W49 .....  | 1441 | 20.68       | ...         | 18.79       | 694.42 | 477.85 | 1".4 | faint UVE          |
| W51 .....  | 1646 | 21.08       | ...         | 19.48       | 678.11 | 443.09 | 0".8 | faint UVE          |
| W54 .....  | 1146 | 19.36       | ...         | 15.50       | 733.57 | 526.64 | 0".1 |                    |
| W55 .....  | 2121 | 18.79       | ...         | 16.85       | 741.28 | 360.81 | 1".1 | BSS-37             |
| W55 .....  | 2141 | 20.88       | ...         | 18.81       | 721.60 | 358.50 | 1".5 | faint UVE          |
| W73 .....  | 2307 | 19.97       | 18.85       | 18.33       | 190.41 | 326.10 | 1".3 | faint UVE          |
| W75 .....  | 1798 | 18.05       | 18.03       | 17.16       | 303.81 | 416.16 | 0".7 | UVE-2, V36         |
| W77 .....  | 945  | 19.80       | ...         | 21.97       | 588.24 | 565.99 | 0".9 | WD-9               |
| W80 .....  | 819  | 20.88       | ...         | 19.16       | 728.91 | 595.90 | 0".2 | faint UVE          |
| W80 .....  | 882  | 20.87       | ...         | 20.49       | 698.91 | 580.20 | 1".4 | faint UVE          |
| W98 .....  | 3259 | 19.82       | 20.84       | 21.95       | 427.11 | 144.16 | 1".1 | WD-10              |
| W98 .....  | 3099 | 21.45       | 20.58       | 19.17       | 423.93 | 176.73 | 0".7 | faint UVE          |
| W105 ..... | 225  | 20.13       | ...         | 19.64       | 122.93 | 735.11 | 1".0 | UVE9               |

NOTE.—The last two columns give the nominal angular separation and a classification/name for the X-ray source or the UV object.

association (proposed by VH98) between V2 and X19 (W30 in the G01 list), and we propose (in agreement with G01) the association of V3 and X10 (W27 in the G01 list). Other position-wise associations appear possible from our data set

(see Table 5 for the complete list). In particular, these are the ones between (1) UVE-2 (the bright blue object discussed in § 3.3) and the X-ray source W75, (2) AKO 9 (BSS-26 in our list; see § 3.1) and source W36, and (4) UVE-6 and UVE-9 and sources W34 and W105, respectively.

However, it should be noted that all the positions of the putative optical counterparts could be still affected by residual uncertainties, since the shifts applied to match the V1/X9 pair represent only a first-order correction. Even though, establishing a physical connection supported only on the positional coincidence is risky, especially because of the large number of peculiar objects found in the crowded core of 47 Tuc. In view of all these caveats, we conservatively conclude that the identifications proposed here are possible and, as such, useful references for future investigations, but not conclusive.

#### 4.2. MSPs

Freire et al. (2001) have recently published accurate timing positions (typical uncertainty less than 0".1) for 15 MSPs in the core of 47 Tuc. Eight of these pulsars have been found in binary systems and, of these, three (namely, MSP-I, MSP-O, and MSP-T) lie in the PC field of view. Exchange interactions in the core of the cluster could in principle produce a significant number of systems comprising a MSP and a main-sequence star. If the MSP is an active X-ray source, its energy emission could also affect such a not-degenerate companion, perhaps making it a blue source. For this reason we cross-correlated the MSP positions with our master source list, and we have found inter-

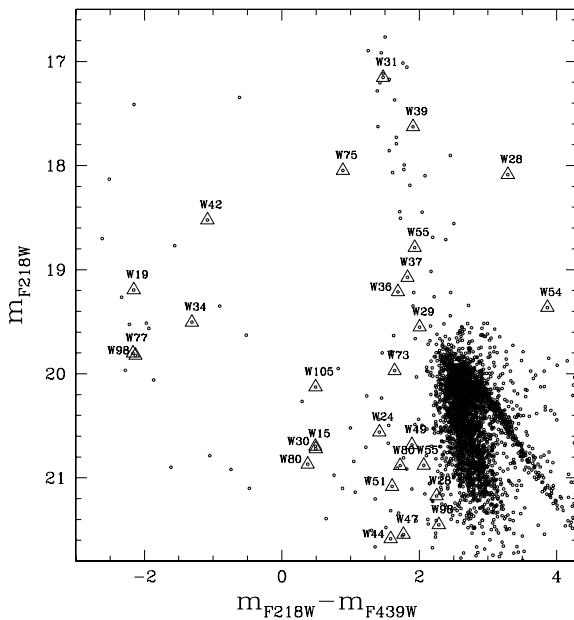


FIG. 4.—Zoom of the ( $m_{F218W}$ ,  $m_{F218W} - m_{F439W}$ ) CMD of Fig. 2. The optical counterpart candidates to the *Chandra* X-ray source are marked with large open triangles and labeled with their names (from Table 1 by G01).

esting matches both with the *Chandra* X-ray source and the UV object lists. First, we confirmed the finding by G01 that three *Chandra* sources (namely, W19, W105, and W39) are nearly coincident with the three binary MSPs (MSP-I, MSP-T, and MSP-O, respectively) lying in the PC field of view. In addition, we found interesting matches with peculiar blue objects. In particular, MSP-I is at 1".8 from a white dwarf (WD-4) and MSP-T is nearly coincident (at only 0".9) with a faint ultraviolet excess object (UVE-9). The case of MSP-O is more complex. Only a TO star (namely, No. 2167) has been found at 0".4 from the nominal position of this MSP. However, MSP-O is located in the region of the peculiar binary AKO 9 (BSS-26 in our list, see § 3.1). Unfortunately, this objects is relatively far away ( $\sim 2''$ ) from the nominal position of MSP-O to be considered a promising optical counterpart candidate to this MSP. Moreover, the matching with the X-ray *Chandra* catalog suggests that AKO 9 is nearly coincident with another *Chandra* source: W36 (see Table 5). Thus, the physical association between MSP-O and the peculiar binary AKO 9 appears unlikely. On the other hand, the only other blue object found in its vicinity (at  $\sim 1''.5$ ) is AKO 6 (which corresponds to BSS-2 in our list). This object did not show significant variability, since it is not coincident with any of the 13 variables detected by E96.

The case of a possible association between MSP-I and WD-4 is probably the more intriguing since MSP companions in binary systems are indeed expected to be WDs (e.g. see the reviews of Verbunt 1993 and Phinney & Kulkarni 1994), with cooling ages longer than at least a few  $10^8$  yr (Hansen & Phinney 1998). According to its position along the WD cooling sequence, WD-4 seems to be a quite young object, approximately  $10^6$  yr old. It is thus unlikely that it is the companion to MSP-I. Although the irradiation of the surface layers of the WD by the MSP beam could modify its photometric properties, making it brighter and slightly bluer (e.g., D'Antona 1995 for a review) and eventually producing an apparent rejuvenation, this would require an unlikely variation of 4–5 mag to reconcile the cooling age of WD-4 with the expected cooling age for a typical MSP companion. Moreover, the induced brightening of the WD should be recognizable by a strong modulation in its light curve, while its heated surface rotates in and out of the line of sight (see, e.g., Stappers et al. 1999). Conversely, from the analysis of the F218W images we have not found any evidence for luminosity variation larger than a few tenths of magnitude for WD-4. However, it should be noted that the images analyzed here do not allow a proper time coverage of the orbital period of the MSP-I system. In fact, the F218W images cover less than  $\sim 16\%$  of the  $P \sim 5.5h$  period estimated by Freire et al (2001). For this reason, we cannot exclude variability for this system.

Finally, UVE-9 is closely blended with a main-sequence star, and its photometry turns presently to be too uncertain for allowing further speculations.

Table 6 lists the absolute positions for the three MSPs and for the blue sources lying nearby. However, in none of the above cases the positional coincidence alone is an argument strong enough to support the identification. Indeed, astrophysical and statistical considerations suggest that all of the above positional coincidences are probably due to chance, and thus probably the optical counterparts to these MSPs are much fainter than the detection limit of the observations analyzed here.

TABLE 6  
MSP AND BLUE OBJECT POSITIONS IN 47 Tuc<sup>a</sup>

| Name              | $\alpha_{2000}$ | $\delta_{2000}$ | $d$  |
|-------------------|-----------------|-----------------|------|
| MSP-I (W19).....  | 00 24 07.93     | −72 04 39.66    | ...  |
| WD-4 .....        | 00 24 07.97     | −72 04 38.80    | 0".8 |
| MSP-T (W105)..... | 00 24 08.55     | −72 04 38.90    | ...  |
| UVE-9 .....       | 00 24 08.73     | −72 04 39.24    | 0".9 |
| MSP-O (W39) ..... | 00 24 04.65     | −72 04 53.75    | ...  |
| BSS-2 .....       | 00 24 04.48     | −72 04 54.99    | 1".5 |
| MSP-L .....       | 00 24 03.77     | −72 04 56.91    | ...  |
| BSS-29 .....      | 00 24 04.07     | −72 04 58.10    | 1".7 |
| MSP-F (W77) ..... | 00 24 03.85     | −72 04 42.80    | ...  |
| WD-9 .....        | 00 24 03.97     | −72 04 43.56    | 0".9 |

NOTE.—Units of right ascension are hours, minutes, and seconds, and units of declination are degrees, arcminutes, and arcseconds.

<sup>a</sup> The name of the *Chandra* X-ray source possibly associated with each MSP is reported in parenthesis.

The probabilities of a physical connection between these three binary MSP systems and the blue objects in their proximity are further reduced if one examines also the optical sources located in the vicinity of the *single, isolated*, MSPs detected in the core of 47 Tuc and included in the field of view covered by the PC. Although no optical counterpart is expected for these objects, it appears (see Table 6) that two of them (over the three nonbinary MSPs listed by Freire et al. 2001), namely, MSP-F and MSP-L, are positionally coincident, within the above uncertainties, with WD-8 and BSS-29, respectively.

While reaching fainter limiting magnitudes would certainly help the search to MSP companions, the current uncertainties on the absolute PC astrometry would still represent the major problem, suggesting that even the availability of much deeper exposures would not solve the ambiguities. We can use equation (1) to compute the expected number of WD (younger than a given cooling time) lying in the fraction of the 47 Tuc core covered by the PC. In doing this, we assumed a WD cooling age of 1 Gyr, i.e., at the median of the WD cooling age distribution of  $\sim 10^8$ – $10^{10}$  yr, as suggested by some WD + MSP systems studied in the field (see Hansen & Phinney 1998; Schönberner, Driebe, & Blöcker 2000). Adopting the Wood (1995) models, this cooling age corresponds to an absolute magnitude  $M_V \sim 13$  (which yields  $m_{F218W} \sim 27$  at the distance of 47 Tuc). Under these assumptions, equation (1) gives a total of  $\sim 1000$  WDs with  $m_{F218W} \lesssim 27$ . Assuming that  $\sim 2''$  is the typical uncertainty in registering the MSP coordinates on the PC frame, the previous number implies an average of six WDs brighter than  $m_{F218W} = 27$  within the uncertainty region. The situation can certainly improved by obtaining a new astrometric solution for the PC using the GSC2.2 (McLean et al. 2001), which has an average absolute astrometric accuracy of  $\sim 0''.5$ , i.e., three times better than the one of the GSC1.1. However, even a remarkable improvement of a factor of 3 in the absolute astrometry of the PC will reduce the probability of a chance coincidence between the MSP and a 1 Gyr-old WD, only to a  $\sim 70\%$ , still too high to claim a position-wise identification.

In summary, the conspiracy of the overcrowded field in the core of 47 Tuc and the extreme faintness of the expected optical counterpart (an old WD) of the companion to a MSP makes extremely difficult a firm identification using



only photometric colors and positioning. Further hints will be necessary, such as the discovery of photometric modulations due to orbital motion, peculiarities in the optical and UV companion candidate spectra, and/or emissivity at other wavelengths.

### 5. CONCLUSIONS

Using data collected with the Planetary Camera of *HST*, we have more than doubled the sample of blue stragglers detected in the core of the globular cluster 47 Tuc and have reported on the discovery of a large number of UV stars, with the hottest of them being probably young WDs. The others UV objects are anomalous UV-excess stars whose true nature and evolution cannot be satisfactorily assessed yet. In fact, many different evolutionary mechanisms involving stellar collisions and interactions could account for them. High-resolution, deeper imaging, and spectroscopic observations in the UV (as those preliminary presented by Knigge et al. 2001) are required to discriminate among the

various models. However, the large number of positional coincidences with X-ray sources (from the recent *Chandra* catalog) indeed suggests that part of them could be IBs. In particular, a significant number of X-ray sources ( $\sim 30\%$ ) have been found to be possibly associated with the faint UVE population discovered here, supporting the presence of a large population of faint CV in the core of this cluster.

We have also explored the possibility of identifying some of the detected blue objects as the optical counterparts to millisecond pulsar companions hosted in the core of the cluster. However, although a few positional coincidences have been found, none of them is suggestive yet of a physical association.

The financial support of the Agenzia Spaziale Italiana (ASI) and of the Ministero della Università e della Ricerca Scientifica e Tecnologica (MURST) to the project Stellar Dynamics and Stellar Evolution in Globular Clusters is kindly acknowledged.

### REFERENCES

- Albrow, M. D., et al. 2001, preprint (astro-ph/0105441)  
 Auriere, M., Koch-Miramond, L., & Ortolani, S. 1989, *A&A*, 214, 113  
 Bailyn, C. D. 1995, *ARA&A*, 33, 133  
 Buonanno, R., Buscema, G., Corsi, C. E., Ferraro, I., & Iannicola, G. 1983, *A&A*, 126, 278  
 Camilo, F., Lorimer, D. R., Freire, P., Lyne, A. G., & Manchester, R. N. 2000, *ApJ*, 535, 975  
 Carson, J. E., Cool, A. M., & Grindlay, J. E. 2000, *ApJ*, 532, 461  
 Castellani, M., & Castellani, V. 1993, *ApJ*, 407, 649  
 Cool, A. M., Grindlay, J. E., Cohn, H. N., Lugger, P. J., & Bailyn, C. D. 1998, *ApJ*, 492, L75  
 Cool, A. M., Grindlay, J. E., Cohn, H. N., Lugger, P. J., & Slavin, S. D. 1995, *ApJ*, 439, 695  
 D'Antona, F. 1996, in *Evolutionary Processes in Binary Stars*, ed. R. A. M. J. Wijers & M. B. Davies (NATO ASI Ser. C, 477; Dordrecht: Kluwer), 287  
 De Marchi, G., Paresce, F., & Ferraro, F. R. 1993, *ApJS*, 85, 293 (DPF93)  
 Di Stefano, R., & Rappaport, S. 1994, *ApJ*, 437, 733  
 Edmonds, P. D., Gilliland, R. L., Guhathakurta, P., Petro, L. D., Saha, A., & Shara, M. M. 1996, *ApJ*, 468, 214 (E96)  
 Edmonds, P. D., Grindlay, J. E., Cool, A., Cohn, H., Lugger, P., & Bailyn, C. 1999, *ApJ*, 516, 250  
 Fabian, A., Pringle, J., & Rees, M. 1975, *MNRAS*, 172, 15  
 Ferraro, F. R., Paltrinieri, B., & Cacciari, C. 1999a, *Mem. Soc. Astron. Italiana*, 70, 599  
 Ferraro, F. R., et al. 1997a, *A&A*, 324, 915  
 Ferraro, F. R., Paltrinieri, B., Fusi Pecci, F., Rood, R. T., & Dorman, B. 1998, in *Ultraviolet Astrophysics—Beyond the IUE Final Archive*, ed. R. González-Riestra, W. Wamsteker, & R. A. Harris (ESA: Noordwijk), 561  
 Ferraro, F. R., Paltrinieri, B., Fusi Pecci, F., Dorman, B., & Rood, R. T. 1997b, *MNRAS*, 292, L45  
 Ferraro, F. R., Paltrinieri, B., Paresce, F., & De Marchi, G. 2000a, *ApJ*, 542, L29  
 Ferraro, F. R., Paltrinieri, B., Rood, R. T., & Dorman, B. 1999b, *ApJ*, 522, 983  
 Ferraro, F. R., Paltrinieri, B., Rood, R. T., Fusi Pecci, F., & Buonanno, R. 2000b, *ApJ*, 537, 312  
 Freire, P. C., Camilo, F., Lorimer, D. R., Lyne, A. G., Manchester, R. N., & D'Amico, N. 2001, *MNRAS*, 326, 901  
 Gilliland, R. L., Bono, G., Edmonds, P. D., Caputo, F., Cassisi, S., Petro, L. D., Saha, A., & Shara, M. M. 1998, *ApJ*, 507, 818  
 Gilliland, R. L., et al. 2000, *ApJ*, 545, L47  
 Geffer, M., Auriere, M., & Koch-Miramond, L. 1997, *A&A*, 327, 137  
 Grindlay, J. E., Heinke, C., Edmonds, P. D., & Murray, S. S. 2001, *Science*, 292, 2290  
 Guhathakurta, P., Yanny, B., Schneider, D. P., & Bahcall, J. N. 1992, *ApJ*, 104, 1790 (G92)  
 Hansen, B. M. S., & Phinney, E. S. 1998, *MNRAS*, 294, 569  
 Holtzman, J. A., Burrows, C. J., Casertano, S., Hester, J. J., Trauger, J. T., Watson, A. M., & Worthey, G. 1995, *PASP*, 107, 1065  
 Hut, P., Murpy, B., & Verbunt, F. 1991, *A&A*, 241, 137  
 Knigge, C., Shara, M. M., Zurek, D. R., Long, K. S., Gilliland, R. L. 2001, preprint (astro-ph/0012187)  
 Lasker, B., et al. 1990, *AJ*, 99, 2018  
 McLean, B., et al. 2001, *Proc. ESO Workshop on Mining the Sky* (Berlin: Springer), in press  
 Minniti, D., Meylan, G., Pryor, C., Phinney, E. S., Sams, B., & Tinney, C. G. 1997, *ApJ*, 474, L27  
 Paltrinieri, B., Ferraro, F. R., Fusi Pecci, F., Rood, R. T., & Dorman, B. 1998, in *Ultraviolet Astrophysics—Beyond the IUE Final Archive*, ed. R. González-Riestra, W. Wamsteker, & R. A. Harris (Noordwijk: ESA), 565  
 Paresce, F., et al. 1991, *Nature*, 352, 297 (P91)  
 Paresce, F., & De Marchi, G. 1994, *ApJ*, 427, L33  
 Paresce, F., De Marchi, G., & Ferraro, F. R. 1992, *Nature*, 360, 46 (PDF92)  
 Paresce, F., De Marchi, G., & Jędrzejewski, R. 1995, *ApJ*, 442, L57  
 Phinney, E. S., & Kulkarni, S. R. 1994, *ARA&A*, 32, 591  
 Renzini, A., & Fusi Pecci, F. 1988, *ARA&A*, 26, 199  
 Richer, H. B., et al. 1997, *ApJ*, 848, 741  
 Schönberner, D., Driebe, T., & Blöcker, T. 2000, *A&A*, 356, 929  
 Shara, M. M., Bergeron, L. E., Gilliland, R. L., Saha, A., & Petro, L. D. 1996, *ApJ*, 471, 804  
 Shara, M. M., & Drissen, L. 1995, *ApJ*, 448, 203  
 Stappers, B. W., van Kerkwijk, M. H., Lane, B., & Kulkarni, S. R. 1999, *ApJ*, 510, L45  
 Verbunt, F. 1993, *ARA&A*, 31, 93  
 Verbunt, F., & Hasinger, G. 1998, *A&A*, 336, 895  
 Wood, M. A. 1995, in *White Dwarfs*, ed. D. Koester